

# Functional Aspects of Intrahepatic Hepatitis B Virus-specific T Cells Induced by Therapeutic DNA Vaccination

Anette Brass<sup>1</sup>, Lars Frelin<sup>1</sup>, David R Milich<sup>2</sup>, Matti Sällberg<sup>1</sup> and Gustaf Ahlén<sup>1</sup>

<sup>1</sup>Department of Laboratory Medicine, Division of Clinical Microbiology, Karolinska Institutet, Karolinska University Hospital Huddinge, Stockholm, Sweden; <sup>2</sup>Vaccine Research Institute of San Diego, San Diego, California, USA

Current therapies for the hepatitis B virus (HBV), a major cause of severe liver disease, suppress viral replication but replication rebounds if therapy is withdrawn. It is widely accepted that immune activation is needed to control replication off-therapy. To specifically activate T cells crossreactive between the hepatitis B core and e antigens (HBcAg/HBeAg) in chronically infected patients, we developed a therapeutic vaccine candidate. The vaccine encompass codon-optimized HBcAg and IL-12 expressing plasmids delivered using targeted high-pressure injection combined with *in vivo* electroporation. One dose of the vaccine primed a B-cell-independent polyfunctional T-cell response, in wild-type, and in HBeAg-transgenic mice with an impaired ability to respond to HBc/eAg. The response peaked at 2 weeks and contracted at week 6 after vaccination. Coadministration of IL-12 improved antibody levels, and T-cell expansion and functionality. The vaccine primed T cells that, 2 weeks after a single dose, cleared hepatocytes transiently expressing HBcAg in vaccinated wild-type and HBeAg-transgenic mice. However, 4 weeks later, these functional responses were lost. Booster doses after 8–12 weeks effectively restored function and expansion of the rapidly contracting T cells. Thus, this vaccine strategy primes functional HBcAg-specific T cells in a host with dysfunctional response to HBV.

Received 28 July 2014; accepted 2 December 2014; advance online publication 6 January 2015. doi:10.1038/mt.2014.233

## INTRODUCTION

The hepatitis B virus (HBV) causes chronic infections that increase the risk for severe liver disease and cancer. Existing nucleoside-based therapies that effectively block the reverse transcriptase (RT) function of HBV decrease the viral load. However, when treatment is stopped, viral replication resume as these drugs are not effective in generating sustained off-therapy responses.<sup>1</sup> It has now been shown that a long-term (>5 years) therapy with these drugs can reduce the risk of cancer.<sup>2</sup> However, with a longer

duration of therapy, the risk for side effects and appearance of drug resistant viral variants increase.<sup>3</sup>

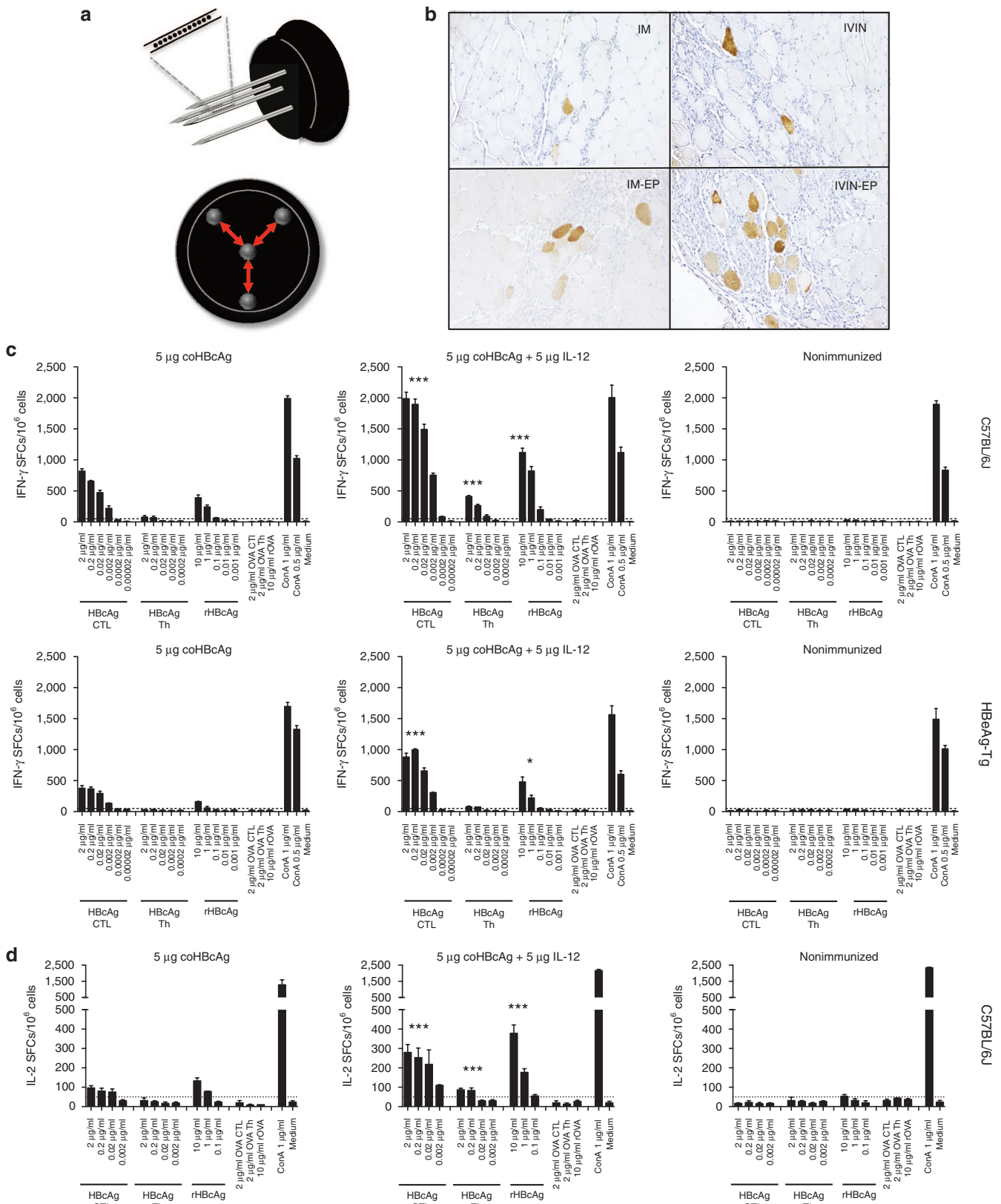
Several studies have highlighted the importance of the host immune response in controlling acute and chronic HBV infections.<sup>4–6</sup> In particular, the spontaneous or interferon-treatment induced control of infection is tightly associated with an increase in the T-cell response to both the hepatitis B core antigen (HBcAg) and hepatitis B e antigen (HBeAg),<sup>7–9</sup> since these two antigens are crossreactive on the T-cell level. Thus, it is likely that T-cell activation is required for a sustained off-therapy response. Early reports of using lamivudine indicated that T-cell responses might be partially restored during lamivudine therapy.<sup>10,11</sup> Although immune responses are likely to recover as viral replication is suppressed, this recovery is not effective enough to achieve off-therapy responses. One explanation may be that the RT inhibitors act during virion maturation by preventing the encapsidated RNA pregenome to be converted to the partially double-stranded DNA. These drugs cannot suppress the production of transcripts and viral antigens from the covalently closed circular (ccc) DNA. Hence, RT inhibitors do not block antigen production in already infected cells, but can reduce the spread of the infection. This is evidenced by a drop in the serum levels of HBV DNA, but not in hepatitis B surface antigen (HBsAg), and a reduced HBcAg-production in the liver.<sup>12,13</sup> However, this does not result in sustained off-therapy responses.

To (re)activate the host immune response, we, and others, have developed therapeutic vaccines for the treatment of chronic infections caused by the HBV and the hepatitis C virus (HCV).<sup>14–18</sup> Therapeutic vaccination alone can transiently activate T-cell responses and decrease viral load in chronically infected humans, albeit to date not sufficiently to sustainably control or clear viral replication.<sup>16,17</sup> Thus, improved vaccines are needed that can activate T cells even in a chronically infected host with a most likely dysfunctional T-cell response to the infecting virus.<sup>19</sup> The goal of a therapeutic vaccine is to induce broad HBV-specific immune responses that help to control the HBV infection.<sup>20,21</sup> This goal is a consequence of the observations that broad, and polyfunctional T-cell responses are important in controlling chronic viral infections.<sup>22,23</sup>

Correspondence: Gustaf Ahlén, Department of Laboratory Medicine, Division of Clinical Microbiology, F68, Karolinska Institutet, Karolinska University Hospital Huddinge, S-141 86 Stockholm, Sweden. E-mail: [gustaf.ahlen@ki.se](mailto:gustaf.ahlen@ki.se)

We have previously shown that the immunogenicity of a DNA-based HBcAg vaccine was effectively enhanced through codon optimization (co) and delivery by *in vivo* electroporation (EP), or electrotransfer (ET).<sup>24</sup> We have also shown that addition

of HBcAg sequences improves the immunogenicity of a HCV nonstructural (NS) 3/4A-based vaccine in a host with impaired immune responses to HCV.<sup>25</sup> We here evaluate several approaches to improve the immunogenicity of a therapeutic vaccine candidate



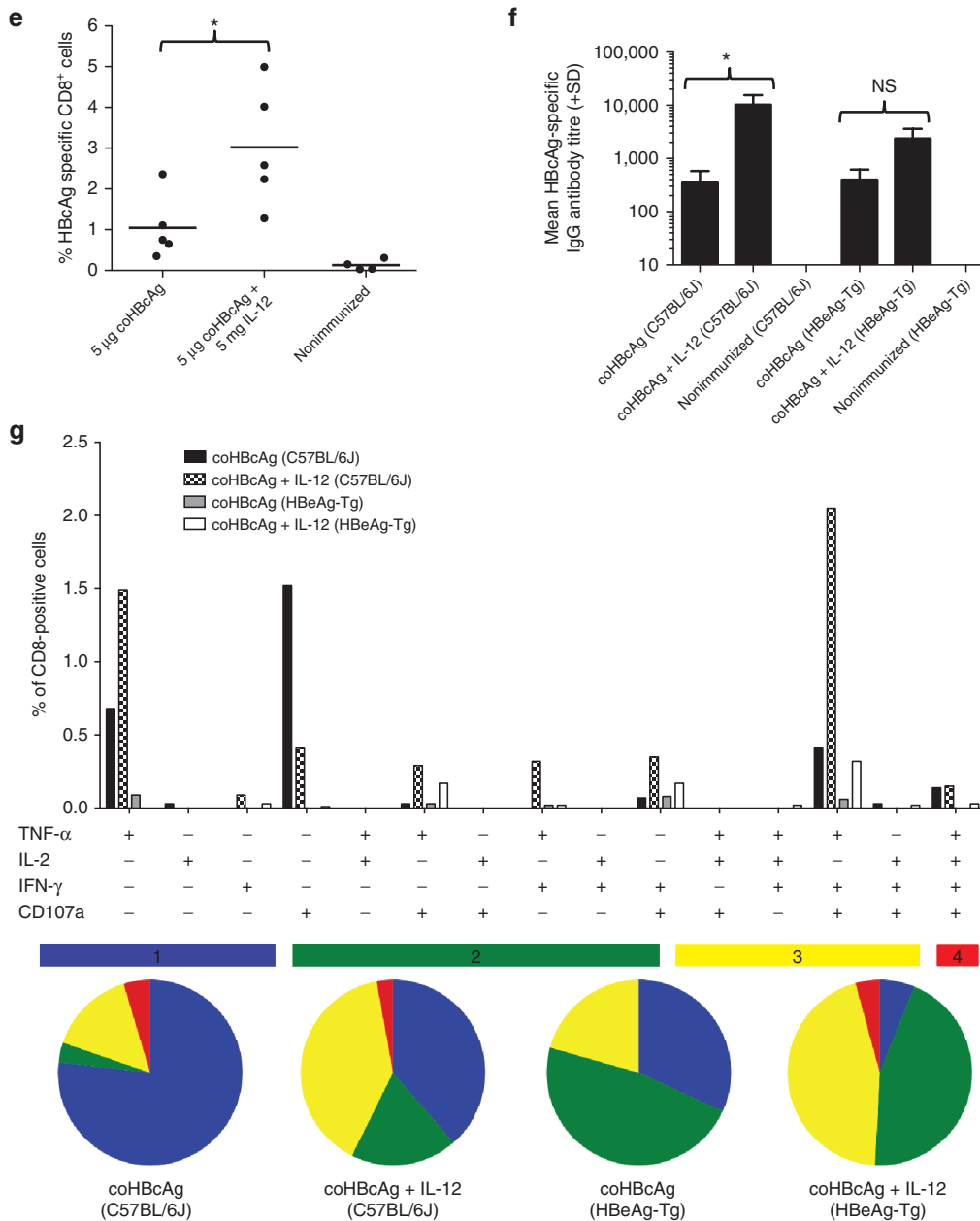


**Figure 1** Codelivery of HBcAg and interleukin (IL)-12 effectively adjuvant HBcAg T-cell responses in C57BL/6J and HBeAg-Tg mice. **(a)** Illustration of the *in vivo* intracellular injection (IVIN) technology with a Y-shaped configuration of the injection needles. The needle ends have been sealed and a number of new holes have been generated along the needle shafts. The red arrows indicate the direction of the injected material. In **(b)** detection of hepatitis C virus nonstructural protein 3 (NS3) expressing muscle fibers in mouse *tibialis cranialis* muscles 72 hours after immunization with 5 µg codon-optimized NS3/4A plasmid DNA is shown. The immunizations have been done using IVIN or a regular needle (IM) with or without *in vivo* EP. **(c,d)** Groups of five C57BL/6J and HBeAg-Tg mice were immunized once with 5µg coHBcAg plasmid DNA alone or in combination with 5 µg IL-12 plasmid DNA by intramuscular immunization with the IVIN technology. The injection area was thereafter electroporated. Two weeks after immunization the mice were bled, sacrificed and splenocytes harvested for determination of T-cell responses. In **(c)**, the number of interferon (IFN)-γ spot forming cells (SFCs) by enzyme-linked immunospot (ELISpot) assay after stimulation with either a CTL peptide (HBcAg CTL), a Th peptide (HBcAg Th) or recombinant HBcAg protein in immunized and nonimmunized C57BL/6J and HBeAg-Tg mice is shown. In **(d)**, the number of IL-2 SFCs in C57BL/6J mice is shown. The ELISpot was detected after *in vitro* stimulation of splenocytes with peptides or recombinant proteins as indicated. Results are given as the mean SFCs/10<sup>6</sup> (+SD) with a cutoff set at 50 SFCs/10<sup>6</sup> splenocytes. Statistical differences have been evaluated between groups of mice immunized with or without IL-12 as \**P* < 0.05, \*\*\**P* < 0.001 using area under the curve (AUC) and analysis of variance (ANOVA). In **(e)**, the expansion of HBcAg-specific CD8<sup>+</sup> T cells was determined using direct *ex vivo* pentamer staining. MGLKFRQL epitope-specific CD8<sup>+</sup> T cells are shown as the percentage of HBcAg-pentamer positive CD8<sup>+</sup> T cells where each filled black circle represent an individual mouse. The black horizontal line indicates the mean of the group. The statistical difference (\**P* < 0.05) was determined using Mann–Whitney *U*-test. **(f)** Shows the mean (+SD) endpoint dilution (three times background value (negative sera)) of anti-HBc IgG antibody titers 2 weeks after last immunization in each group of mice. NS, not significant, indicates no statistical difference, and \**P* < 0.05 (Mann–Whitney *U*-test). **(g)** Polyfunctionality of the HBcAg-specific T-cell responses from groups (five mice/group) of C57BL/6J and HBeAg-Tg mice 2 weeks after immunization with HBcAg DNA with or without IL-12. Splenocytes were stimulated with overlapping peptide pools (covering the full-length HBcAg-protein). Each bar represents the percentage of CD8<sup>+</sup> T cells expressing/producing CD107a, TNF-α, IL-2, and/or IFN-γ 12 hours after antigen stimulation. Each pie chart represent the ratio of the groups number of functions, matched by colors 1 (blue), 2 (green), 3 (yellow), and 4 (red).

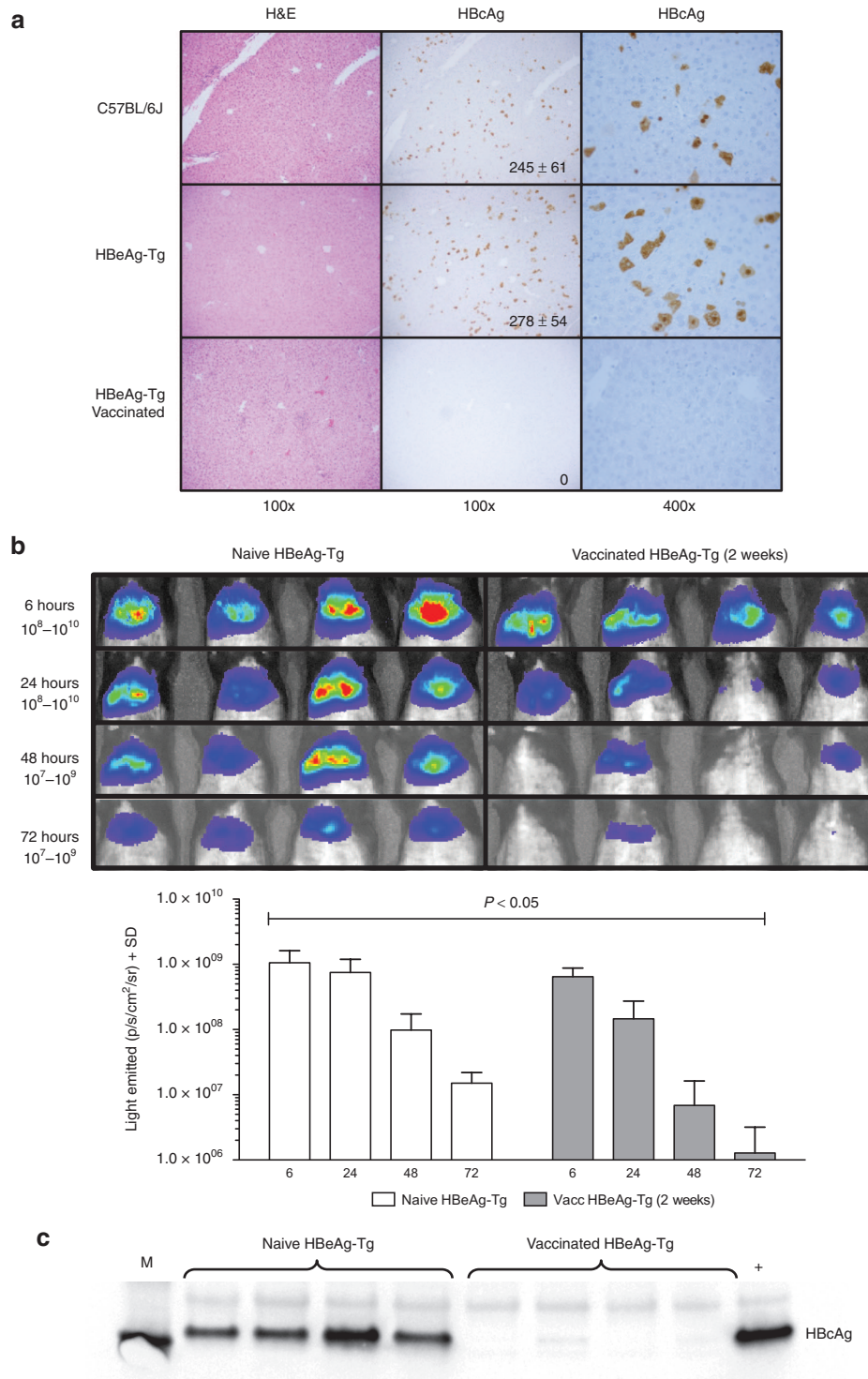


**Figure 2** *In vivo* clearance of HBcAg-expressing hepatocytes. **(a)** Immunohistochemical staining of inflammation (H&E) and kinetics of HBcAg-expression (peroxidase) in mouse livers 72 hours after hydrodynamic challenge with 50  $\mu$ g coHBcAg-pVAX1 and 50  $\mu$ g Luc2-pVAX1. One group of HBeAg-Tg mice was immunized 2 weeks prior to the hydrodynamic challenge using IVIN-EP with 5  $\mu$ g coHBcAg + 5  $\mu$ g IL-12. The number of HBcAg-expressing hepatocytes/15 mm<sup>2</sup> (mean  $\pm$  SD) is given for nonvaccinated C57BL/6J and HBeAg-Tg mice. In **(b)**, the biodistribution of firefly luciferase determined by using *in vivo* imaging (Caliper Life Sciences) is shown in immunized (2 weeks) and nonimmunized HBeAg-Tg mice (four mice/group) 6–72 hours after HBcAg-luciferase transfection of hepatocytes. Statistical difference has been indicated ( $P < 0.05$ ) using area under the curve (AUC) and analysis of variance (ANOVA). **(c)** Detection of HBcAg in livers of mice 72 hours after hydrodynamic injection using immunoprecipitation followed by western blot analysis. Lane 1) Magic Mark, molecular weight marker (Life Technologies), lane 2–5) individual mouse liver samples from nonimmunized HBeAg-Tg, and lane 6–9) individual mouse liver samples from immunized HBeAg-Tg and in lane 10) positive control (*e.g.*, coHBcAg transfected HepG2 cell lysate).

for HBV. For this purpose, we use the HBeAg-transgenic (Tg) mouse model with dysfunctional T-cell responses to both HBcAg and HBeAg. The HBeAg-Tg mice (B10.S-Tg31e lineage on C57BL/6J background) display low-affinity binding of an H-2<sup>b</sup>-restricted Th epitope (129–140) (refs. 26–28). This results in a dysfunctional Th-2-skewed T-cell response toward both HBcAg and HBeAg that can be activated by various immunizations.<sup>26–28</sup> This is therefore a suitable model to evaluate vaccine improvements and the effects of including the antiviral cytokine interleukin (IL)-12, important for viral clearance of HBV and plays a role in shaping the T-cell repertoire.<sup>29,30</sup>

## RESULTS

### Improving DNA vaccine delivery

As a key step in improving immunogenicity of genetic material *in vivo*, we developed a new technology termed *in vivo* intracellular injection (IVIN; **Figure 1**). The IVIN technology is based on a device with multiple needles where several holes (between 72–144 holes depending on the design) have been laser cut along the needle shafts (**Figure 1a**). The idea is to isolate a specific volume of tissue and then overload it with a vaccine-containing solution, similar to a hydrodynamic injection.<sup>31</sup> In the overloaded tissue, the plasmid DNA is more effectively taken up by muscle cells, resulting in an increased expression of the vaccine antigen (**Figure 1b**). In mice, the injection is a forced (19 newton, N) injection of 30  $\mu$ l of plasmid DNA controlled by a spring-loaded device, to obtain a controlled pressure and a high reproducibility (Ahlen *et al.*, unpublished data). To evaluate the IVIN technology, we first used the HCV NS3/4A-based DNA vaccine.<sup>17</sup> NS3 protein-expression was determined in paraffin embedded sections from mouse *tibialis cranialis* muscle tissue from mice immunized using regular intramuscular injection (IM) or the IVIN device alone or in combination with *in vivo* EP (**Figure 1b**). This suggested that the IVIN technology by itself improved transfection efficiency and, importantly, caused local inflammation, as compared to a standard needle injection (**Figure 1b**). The combination of IVIN followed by *in vivo* EP further improved NS3-protein expression (**Figure 1b**). We therefore used the IVIN technology combined with *in vivo* EP in the current study.

### Optimizing the priming milieu

Previous studies where HBcAg has been endogenously expressed through genetic vaccination have shown priming of both humoral and cellular immune responses in mice.<sup>24,32,33</sup> We could show that the ability of endogenous HBcAg to induce cytotoxic T lymphocytes (CTLs) was improved by increasing plasmid uptake and expression levels through *in vivo* EP.<sup>24</sup> To further improve immunogenicity, we here used the IVIN technology combined with *in vivo* EP and evaluated the addition of a plasmid expressing IL-12. The inclusion of IL-12 increased immunogenicity by more than 100% in both wild-type and HBeAg-Tg mice as determined by the number of IFN $\gamma$ -producing cells by enzyme-linked immunospot (ELISpot) (**Figure 1c**). Both CD4<sup>+</sup> Th (HBcAg Th) and CD8<sup>+</sup> CTL (HBcAg CTL) responses were significantly improved in the wild-type mice whereas mainly the CTL responses were improved in the HBeAg-Tg mice. There was a significant increase in the number of IL-2-producing cells in wild-type mice, whereas the overall IL-2 response was low

after a single vaccination in HBeAg-Tg mice (**Figure 1d** and data not shown). Furthermore, a significantly higher frequency of HBcAg-specific CD8<sup>+</sup> T cells, as detected by direct *ex vivo* pentamer staining, was primed using IL-12 in comparison to the HBcAg vaccine alone (**Figure 1e**,  $P < 0.05$ , Mann–Whitney *U*-test). Unexpectedly, also HBcAg-specific IgG antibody levels were improved by IL-12 in both wild-type and HBeAg-Tg mice at 2 weeks after a single immunization, albeit a statistical difference was only observed in wild-type mice (**Figure 1f**,  $P < 0.05$  and NS, Mann–Whitney *U*-test).

### IL-12 improves HBcAg-specific T-cell polyfunctionality

To better characterize the immunogenicity of the HBcAg-based DNA vaccine, the polyfunctionality of the CD8<sup>+</sup> T cells was determined at 2 weeks after a single immunization. This showed that the inclusion of IL-12 increased the proportion of trifunctional HBcAg-specific T cells expressing tumor necrosis factor- $\alpha$  (TNF- $\alpha$ ), IFN- $\gamma$ , and CD107a (**Figure 1g**).

### Vaccine-primed T cells eliminate HBcAg-expressing hepatocytes in HBeAg-transgenic mice

We have previously shown that HBcAg vaccine-primed T cells eliminate HBcAg-expressing hepatocytes in transiently transgenic wild-type mice.<sup>24</sup> We here tested whether vaccine-induced T cells could eliminate hepatocytes expressing HBcAg also in HBeAg-transgenic mice, which have an impaired T-cell response to both HBcAg and HBeAg. The comparison of non-immunized wild-type (245  $\pm$  61) or HBeAg-Tg (278  $\pm$  54), did not reveal any differences. However, HBeAg-Tg mice vaccinated with 5  $\mu$ g HBcAg and 5  $\mu$ g IL-12 2 weeks before the hydrodynamic challenge had completely cleared HBcAg-expressing cells within 72 hours from the hydrodynamic injection (**Figure 2a,c**). Naive and vaccinated HBeAg-Tg mice were challenged with a mixture of HBcAg- and luciferase-expressing plasmid, and at 24–72 hours postchallenge, there was significantly less HBcAg/luciferase detected in the vaccinated HBeAg-Tg mice (**Figure 2b**,  $P < 0.05$ , area under the curve (AUC) and analysis of variance (ANOVA)). Thus, the vaccine-primed, HBcAg-specific T cells were functional *in vivo*.

### Longevity of primed T cells after a single immunization

We now know that a single vaccination induced a rapid expansion of interferon (IFN)- $\gamma$  producing HBcAg-specific T cells. Next, we wanted to determine the longevity of these responses after a single immunization in wild-type mice. Six, 10, and 14 weeks after a single vaccination, the number of IFN- $\gamma$  producing splenic T cells had drastically decreased (**Figure 3a**). In contrast, the anti-HBc IgG antibody responses were maintained or improved at 6, 10, and 14 weeks after a single immunization (**Figure 3b**). Similar to the number of IFN- $\gamma$  producing splenic T cells, the percent polyfunctional (IFN- $\gamma$ <sup>+</sup>, TNF- $\alpha$ <sup>+</sup>, and CD107a<sup>+</sup>) CD8<sup>+</sup> T cells was reduced after 6 weeks and almost absent at 10 and 14 weeks post the single immunization (**Figure 3c**). These results raised the question whether the *in vivo* functionality of the T-cell responses also was lost. We used our transiently transgenic mouse model to generate HBcAg-luciferase expressing hepatocytes in nonimmunized and vaccinated wild-type and HBeAg-Tg mice. Six weeks after a single vaccination,

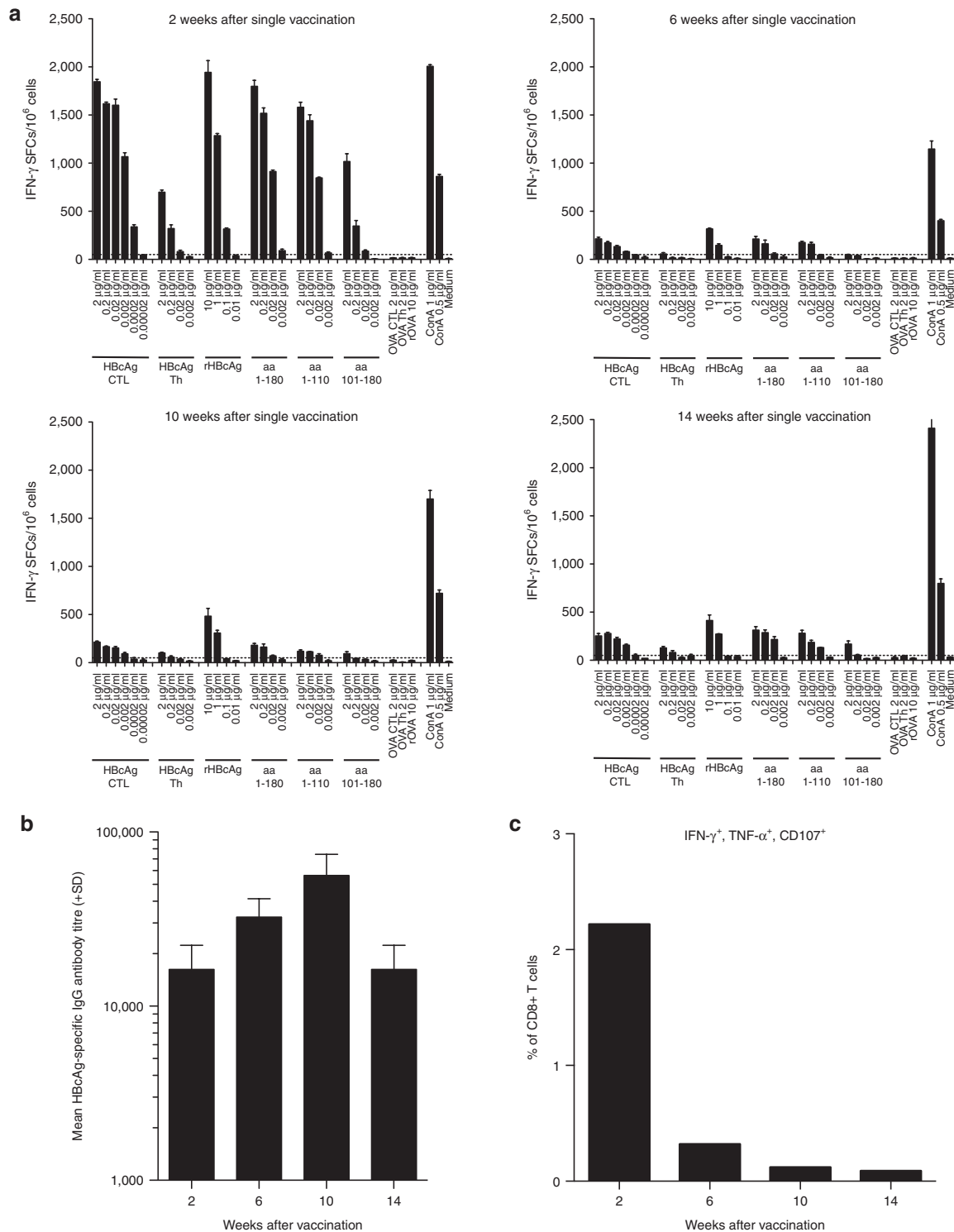


**Figure 3 Rapid loss of T-cell responses after a single immunization.** Groups of five C57BL/6J and HBeAg-Tg mice were immunized once with 5  $\mu$ g coHBcAg plasmid DNA in combination with 5  $\mu$ g IL-12 plasmid DNA by intramuscular immunization (IVIN-EP). Two, 6, 10, or 14 weeks after immunization, the mice were bled, sacrificed, and splenocytes harvested for determination of T-cell responses. In (a), the numbers of IFN- $\gamma$  spot forming cells (SFCs) by enzyme-linked immunospot (ELISpot) assay in immunized C57BL/6J mice are shown. The ELISpot was determined after *in vitro* stimulation of splenocytes with peptides and recombinant proteins as indicated. Results are given as the mean SFCs/ $10^6$  (+SD) splenocytes with a cutoff set at 50 SFCs/ $10^6$  splenocytes. (b) The mean (+SD) endpoint dilution of anti-HBc IgG antibody titers 2, 6, 10, or 14 weeks after a single immunization. (c) Polyfunctionality (IFN- $\gamma^+$ , TNF- $\alpha^+$ , CD107a $^+$ ) of HBcAg-specific T-cell responses of splenocytes stimulated with overlapping peptide pools (0.3  $\mu$ g/ml each peptide) covering the full-length HBcAg-protein. Each bar represents the percentage of CD8 $^+$  T cells that are polyfunctional 12 hours after antigen stimulation.



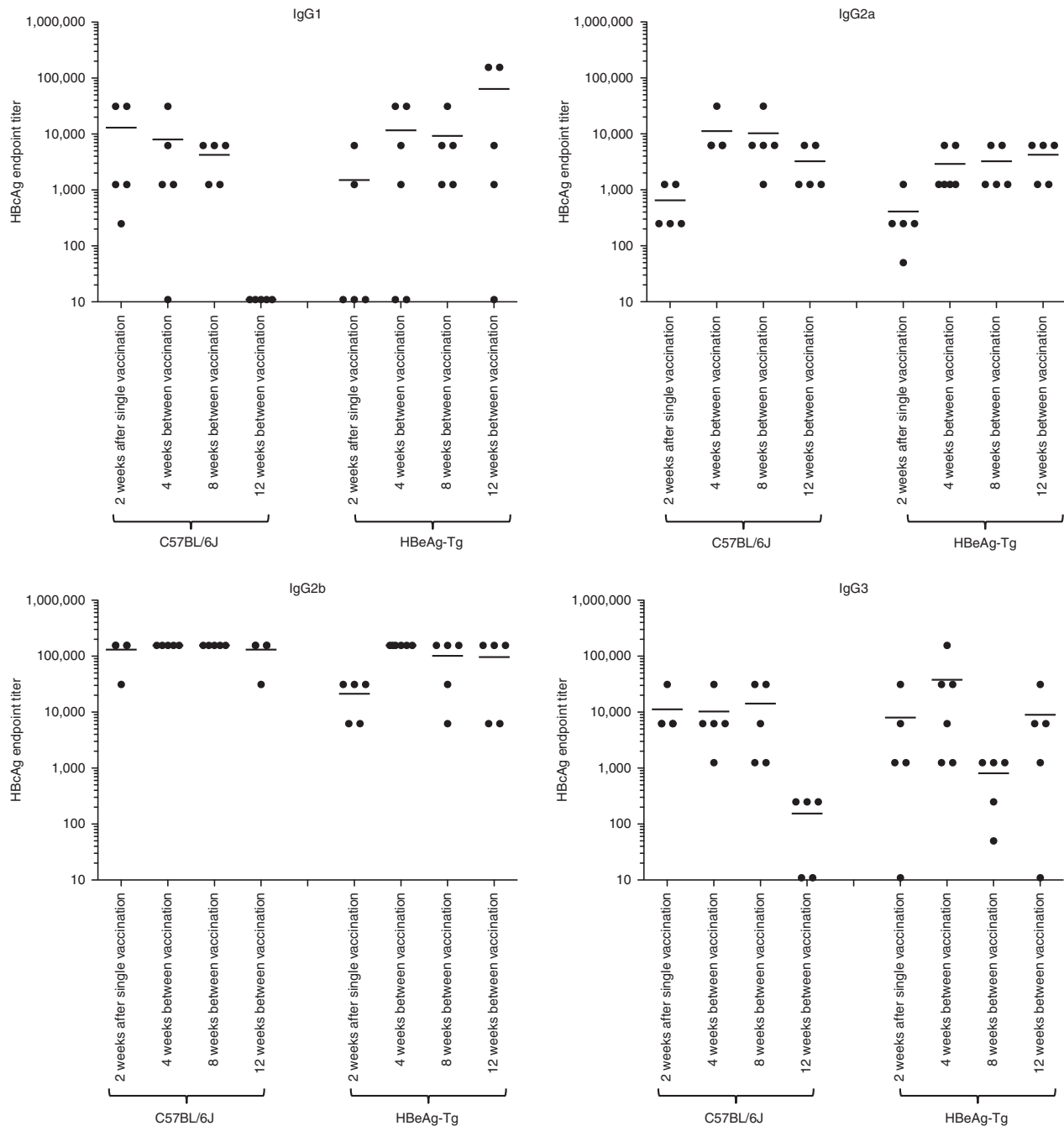


**Figure 5** IgG subclasses in C57BL/6J and HBeAg-Tg mice after one or two immunizations. Groups of five to seven C57BL/6J and HBeAg-Tg mice were immunized once or twice with 5  $\mu$ g coHBcAg plasmid DNA in combination with 5  $\mu$ g IL-12 plasmid DNA by intramuscular immunization (IVIN-EP). The groups of mice that were immunized twice had 4, 8, or 12 weeks between immunizations. Two weeks after last immunization, mice were bled and serum was tested for anti-HBc IgG subclasses (IgG1, IgG2a, IgG2b, and IgG3). All data are given as individual end point titers (black filled circles) with each groups mean titer indicated (line).

the clearance of HBcAg-luciferase expressing hepatocytes was then analyzed kinetically by *in vivo* imaging (**Supplementary Figure S1**). Neither in the vaccinated C57BL/6J nor in the vaccinated HBeAg-Tg mice clearance of HBcAg-luciferase expressing hepatocytes was evident, as compared to the nonvaccinated groups of mice (**Supplementary Figure S1**,  $P =$  nonsignificant (NS), AUC and ANOVA). Thus, the *in vivo* longevity of *in vivo* functional HBcAg-specific T-cell responses after a single immunization is short, and suggests the need for additional booster doses.

### Restoration of functional T-cell and B-cell responses

Since the immune response after a single immunization was short-lived, we determined whether a booster immunization could restore or improve the longevity of these responses. To determine the best timing for the booster dose, we immunized groups of wild-type and HBeAg-Tg mice twice with 4, 8, or 12 weeks between immunizations. The peak number of IFN- $\gamma$  SFCs after peptide stimulation was consistently observed 2 weeks after a single immunization in both wild-type and HBeAg-Tg mice



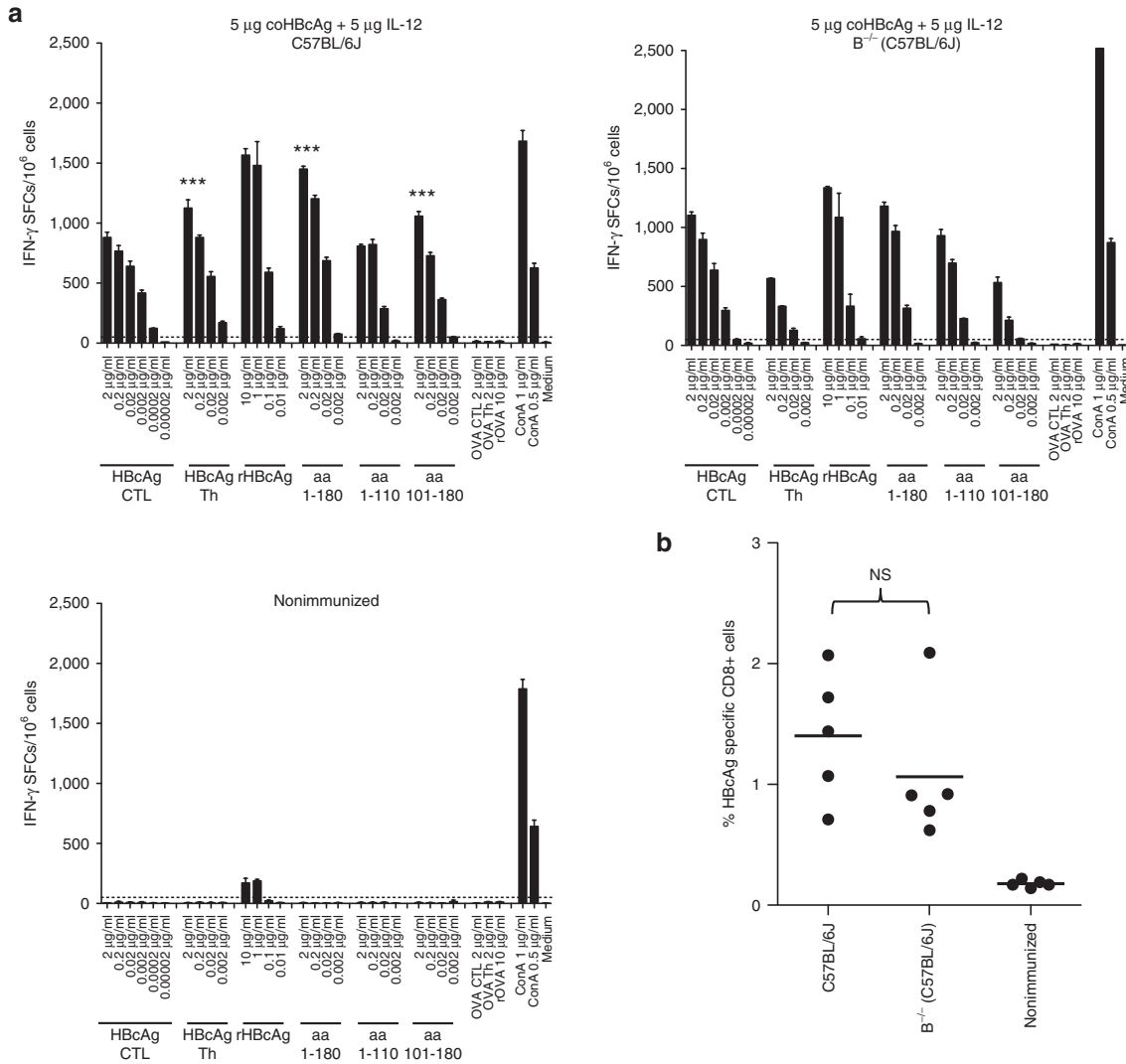


**Figure 6 Priming of T-cell responses is partly independent of B cells.** Groups of five C57BL/6J and  $B^{-/-}$  mice were immunized twice with 5  $\mu\text{g}$  coHBcAg plasmid DNA alone or in combination with 5  $\mu\text{g}$  IL-12 plasmid DNA by intramuscular immunization using regular needle injection in combination with *in vivo* EP. Two weeks after the last immunization, the mice were sacrificed and splenocytes harvested for determination of T-cell responses. The number of IFN- $\gamma$  spot forming cells (SFCs) was determined by enzyme-linked immunospot (ELISpot) assay in the immunized C57BL/6J and  $B^{-/-}$  mice and in C57BL/6J nonimmunized mice as control (**a**). The ELISpot was determined after *in vitro* stimulation of splenocytes with peptides and recombinant proteins as indicated. Results are given as the mean SFCs/ $10^6$  (+SD) splenocytes with a cutoff set at 50 SFCs/ $10^6$  splenocytes. Statistical differences have been evaluated between the two immunized groups of mice as  $***P < 0.001$  using area under the curve (AUC) and analysis of variance (ANOVA). In (**b**), the expansion of HBcAg-specific CD8 $^{+}$  T cells was determined using direct *ex vivo* pentamer staining. MGLKFRQL epitope-specific CD8 $^{+}$  T cells are shown as the percentage of HBcAg-pentamer positive CD8 $^{+}$  T cells where each black filled circle represent an individual mouse. The black horizontal line indicates the mean of the group. There was no statistical difference (NS) between the two immunized groups of mice (Mann-Whitney *U*-test).

(**Figure 4a**). The booster dose restored responsiveness to all tested antigens regardless of the time between doses (**Figure 4a** compared with **Figure 3a**). It is worth noting that the IFN- $\gamma$  response to recombinant HBcAg was restored in the HBcAg-Tg mice after the second vaccine dose to almost the same levels as seen in the wild-type mice (**Figure 4a**). The reason for this is not clear but may indicate activation of novel Th responses. The percent polyfunctional (IFN- $\gamma^{+}$ , TNF- $\alpha^{+}$ , and CD107a $^{+}$ ) CD8 $^{+}$  T cells was comparable at all time points in both the wild-type and HBcAg-Tg mice (**Figure 4b**). The induction of HBcAg-specific IgG antibodies was significantly improved after two immunizations as compared to one vaccination in both wild-type and HBcAg-Tg mice (**Figure**

**4c**,  $P < 0.05$ , Mann-Whitney *U*-test). These data suggest that immune responses against HBcAg can be boosted using repeated immunization strategies.

**Booster vaccinations alter the Th1/Th2-balance as determined by IgG subclass responses**

To further evaluate the effect of the booster response, we characterized anti-HBc IgG subclass distribution in the vaccinated mice (**Figure 5**). All IgG subclasses were detected, with a predominant IgG2b response in both wild-type and HBcAg-Tg mice, an intrinsic property of HBcAg.<sup>34,35</sup> The most obvious effect was seen 2 weeks after a booster immunization as IgG2a increased 1

log in both wild-type and HBeAg-Tg mice, suggesting a Th1-like response. A booster dose at 12 weeks induced a profound Th1 skewing of the response in wild-type mice with the disappearance of IgG1 and an almost 2-log drop in IgG3.

The situation was slightly different in the HBeAg-Tg mice, known to be Th2-like in their response to HBeAg.<sup>28</sup> In these mice, all HBeAg-specific IgG subclasses increase after the booster dose, with the exception of IgG3 (Figure 5). Again, IgG2b was the dominating IgG subclass.

### Role of B cells in the priming of HBeAg-specific T cells

B cells have been proposed as the primary antigen presenting cell (APC) for exogenous/extracellular HBeAg, which may or may not be the case for endogenous/intracellular HBeAg.<sup>32</sup> With this in mind, it is easy to envision that, at the time of a booster dose, the high levels of anti-HBe should minimize the role of B cells as APCs. To further test whether B cells play a role in T-cell priming following DNA-based vaccination with HBeAg, we determined the priming and expansion of HBeAg-specific T cells in wild-type and B-cell-deficient ( $B^{-/-}$ ) mice primed and then boosted 4 weeks later. There was no difference in HBeAg-specific CTL production of IFN- $\gamma$  or the number of HBeAg-specific CD8<sup>+</sup> T cells between the wild-type and the  $B^{-/-}$  mice (Figure 6a,b,  $P = NS$  ( $P = 0.4206$ , Mann-Whitney  $U$ -test)). However, the responses to the Th peptide, and peptide pools containing the same Th epitope (peptide pools aa 1–180 and aa 101–180), were significantly higher in the C57BL/6J mice as compared to the  $B^{-/-}$  mice (Figure 6a,  $P < 0.001$ , AUC-ANOVA). This suggests that the priming and expansion of HBeAg-specific T helper cells, but not CTLs, is influenced by B cells and/or the presence of pre-existing anti-HBe after a DNA-based immunization with HBeAg.

## DISCUSSION

There is little doubt that some sort of immune therapy that can adjuvant the current direct acting antivirals is needed for chronic HBV infections. Several studies have investigated HBeAg as a potential genetic- or protein-based vaccine.<sup>32,36,37</sup> A key feature needed in an HBeAg-specific therapeutic vaccine for chronic HBV is the ability to induce strong and durable T-cell responses. To optimize the immunogenicity of DNA vaccines, several approaches have been evaluated. We have shown that codon optimization of the HBeAg-based DNA vaccine combined with delivery by *in vivo* EP greatly improved immunogenicity of a single DNA dose.<sup>24</sup> As immunogenicity is pivotal for the success of a DNA vaccine, we wanted to improve on the vaccine further in a mouse model with dysfunctional T-cell responses to HBeAg and HBeAg. These types of models better resemble the situation in humans with chronic HBV infection. We here used the HBeAg-Tg mice, which have a dysfunctional T-cell response to HBeAg and HBeAg.<sup>27</sup> However, they are not completely tolerant and display low-avidity response to an H-2<sup>b</sup>-restricted Th epitope (129–140) reflected in a Th2-skewing of the response.<sup>27,28</sup>

As we clearly show in this paper, the priming of HBeAg-specific CTL responses is also impaired in these HBeAg-Tg mice, revealing a dysfunction also in CD8<sup>+</sup> T-cell repertoire. Hence, this is a useful model to study vaccine-induced immune responses. To

improve the vaccine, we here optimize the priming milieu at the injection site by coadministration of cytokines. IL-12 is important for an effective induction and maturation of vaccine-induced CTLs.<sup>30,38,39</sup> We found that the inclusion of an IL-12 expressing plasmid promoted the priming of HBeAg-specific T-cell responses, evidenced by a higher level of IFN- $\gamma$  production and a greater number of HBV-specific CD8<sup>+</sup> T cells. As the quality of HBV-specific T cells seems important for the outcome of the disease,<sup>20</sup> we also investigated the polyfunctionality of the vaccine primed T cells. Inclusion of IL-12 increased the proportion of trifunctional (IFN- $\gamma$ <sup>+</sup>, TNF- $\alpha$ <sup>+</sup>, and CD107a<sup>+</sup>) CD8<sup>+</sup> T cells in both wild-type and HBeAg-Tg mice. The cells were indeed functional, since vaccine-primed T cells eradicated HBeAg-expressing liver cells in HBeAg-Tg mice. This is important since the HBeAg-Tg mice are prone to mount a Th2-skewed immune response that counteracts the priming of antiviral Th1-responses.<sup>28</sup> Thus, we can prime intrahepatic functional T cells in the HBeAg-Tg mouse model that better mimics the defective T-cell responses normally seen in individuals with chronic HBV.

*In vivo* EP is an effective way to improve uptake and expression of vaccine antigens resulting in improved T-cell priming.<sup>24,40,41</sup> To further improve delivery and uptake of DNA vaccines, we used the new IVIN technology that overloads a targeted volume of tissue with genetic material. By combining the IVIN technology with *in vivo* EP, we improved vaccine expression and specific immune responses (current paper and Ahlén *et al.*, unpublished data). Thus, this is certainly a promising combination for DNA vaccine delivery.

As expected, we noted that the primed HBeAg-specific responses contracted following a single dose, and therefore, we examined the best spacing between immunizations. The vaccine-induced immune response after a single immunization contracted between 2 and 6 weeks from immunization, as evidenced by both cytokine production and *in vivo* functionality. A booster dose immunization given after 4, 8, or 12 weeks effectively restored the immune response. However, the same levels of T-cell activation as seen 2 weeks after the first immunization were not achieved. Several other studies have shown that heterologous prime-boost vaccination strategies are effective in boosting HBV-specific immune responses.<sup>36,42,43</sup> However, these vaccine strategies are more complex since they depend on several different vaccine antigens and delivery technologies. A homologous vaccine approach, such as described herein, is easier to move to clinical trials and more eligible for global distribution.

We used the anti-HBe IgG subclass distribution as an additional indicator of the primed Th-phenotype. We found that the most profound Th1-skewing was seen when the booster dose was given at week 12, evidenced by the loss of the Th2-driven IgG1 subclass in wild-type mice. In the HBeAg-Tg mice, there was an increase in all IgG subclasses, except for IgG3. Thus, despite a booster dose including the IL-12 plasmid, no major changes in the IgG subclass profile was seen in the Tg mice with a dysfunctional T-cell response to HBeAg.

Since B cells have been shown to play a pivotal role in the priming of CD4<sup>+</sup> T cells, we asked whether they also play a role in the priming of HBeAg-specific CTLs, or if this can be contributed to other APCs such as dendritic cells or macrophages.<sup>44</sup> Two

DNA-based vaccinations of wild-type and B-cell-deficient mice confirmed that B cells were pivotal for HBcAg-specific Th-cell activation, but had no or a limited effect in CTL priming. Overall, this suggests that B cells are important in mounting a complete and broad HBcAg-specific response, and that pre-existing anti-HBc most likely has no adverse effects on T-cell priming.

In conclusion, we have shown that repeated vaccinations with a combination of a codon-optimized HBcAg gene with an IL-12 expressing-plasmid using a targeted delivery effectively primes a T-cell response that is functional in the liver of a host with a dysfunctional T-cell response to HBc/eAg. These observations are useful for the development of a potent therapeutic vaccine for chronic hepatitis B.

## MATERIALS AND METHODS

**Animals.** Inbred C57BL/6J (H-2<sup>b</sup>), HBcAg-transgenic (HBcAg-Tg) (H-2<sup>b</sup>) and B cell *-/-* (B6.129S2-*Ighmtm1Cgn/J*) (H-2<sup>b</sup>) mice were housed at Karolinska Institutet, Division of Comparative Medicine, Clinical Research Center, Karolinska University Hospital Huddinge, Stockholm, Sweden. The HBcAg-Tg mice originate from the B10.S-Tg31e lineage<sup>26,27</sup> and express the HBcAg subtype *ayw* under the control of the metallothionein promoter, inducing a T-cell dysfunction to HBc/eAg.<sup>27,34</sup> The animals were either purchased (Charles River Laboratories, Sulzfeld, Germany) or bred in-house. The animals were caged at 5–10 mice per cage and fed with a commercial diet (RM3 (p) PL IRR diet; Special Diet Service) with free access to food and water. All animals were 6–24 weeks of age at the start of the experiment. All experimental protocols involving animals were approved by the Ethical Committee for Animal Research at Karolinska Institutet.

**Plasmid DNA.** The codon-optimized (co) HBcAg-pVAX1 plasmid (GenBank accession number DI244925.1 (<http://www.ncbi.nlm.nih.gov/genbank>)) has been described previously.<sup>32</sup> Mouse IL-12 (pORF-mIL-12) was purchased from InvivoGen (San Diego). The FLuc2-gene (Promega, Madison, WI) cloned into pVAX1 has been described previously.<sup>31</sup> Plasmids were grown in competent TOP10 *Escherichia coli* (Life Technologies, Carlsbad, CA) and purified using Qiagen EndoFree Plasmid purification Kit according to the manufacturer's instructions (Qiagen, Hilden, Germany). Plasmid DNA concentration was determined spectrophotometrically and the purified DNA was dissolved in sterile phosphate-buffered saline at concentrations of 2 mg/ml. Restriction enzyme digest were performed to ensure that the plasmid contained the gene of interest with the correct size. All DNA plasmids were sequenced to ensure correct nucleotide sequence (Eurofins MWG Operon, Ebersberg, Germany).

**Peptides and antigens.** A total of eighteen 20-mer peptides (each having 10 amino acid (aa) overlap) covering the HBcAg aa 1–180, derived from the full-length HBcAg protein were purchased from Sigma Aldrich (St Louis, MO). To be able to study both CD4<sup>+</sup> and CD8<sup>+</sup> T-cell responses in detail, we use two previously identified HBcAg H-2<sup>b</sup> restricted epitopes, the HBcAg-Th peptide (H-2IA<sup>b</sup> aa sequence: PPAYRPPNAPIL (HBcAg aa 129–140)), and the HBcAg-CTL peptide (H-2K<sup>b</sup> aa sequence: MGLKFRQL (HBcAg aa 93–100)). The following non-HBV control peptides were used; SIINFEKL (OVA 257–264, CTL-epitope) and ISQAVHAAHAEINEAGR (OVA 323–339, Th-epitope) were synthesized by automated peptide synthesis as described previously (ChronTech Pharma AB, Huddinge, Sweden).<sup>45</sup> Recombinant HBcAg-protein (aa 1–183) was produced in *E. coli* and kindly provided by Darrell Peterson (Virginia Commonwealth University, Richmond, VA). Chicken egg albumin (OVA), and Concanavalin A (ConA) were purchased from Sigma Aldrich.

**IVIN device for delivery of DNA vaccine.** Immunizations in this study were performed with the IVIN delivery device (unless otherwise stated) (Ahlén *et al.*, unpublished data). Briefly, the IVIN is a multineedle injection device

where the sharp end of the needles has been sealed and several (12–36) new 0.05 mm holes in diameter have been laser cut along the needle shaft of each needle. The IVIN device used in this study consists of four needles arranged in a Y-shaped formation with all the holes facing a central point (Figure 1a). The injection is a forced injection of 30 µl plasmid DNA controlled by the spring-loaded device. By using the IVIN device, an isolated area of the muscle tissue can be overloaded with the vaccine solution.

**Immunization protocol and in vivo bioluminescence imaging.** Mice were immunized intramuscularly in the tibialis cranialis muscle with 5 µg plasmid DNA coHBcAg-pVAX1 alone or in combination with 5 µg mIL-12-pORF1 in a volume of 30 µl using the *in vivo* injection device (IVIN) or by regular needle injection. Immediately following administration of the plasmid DNA, tibialis cranialis muscles were subsequently electroporated (EP) using the Cliniporator<sup>2</sup> device (IGEA, Carpi, Italy) with a 1 ms 600 V/cm pulse followed by a 400 ms 60 V/cm pulse pattern.

Transient expression of HBcAg and luciferase in the livers of mice was achieved by hydrodynamic injection. A total volume of 1.8 ml (8% of body weight) Ringers solution containing 50 µg coHBcAg-pVAX1 and 50 µg Luc2-pVAX1 plasmid DNA was injected intravenously in the tail vein within 5 seconds. The presence of luciferase reporter gene expression was determined at 6, 24, 48, and 72 hours by bioluminescence in anaesthetized mice using the IVIS Spectrum *in vivo* imaging system (Caliper Life Sciences, Hopkinton, MA). To detect the presence of reporter gene expression the luciferin substrate (Caliper Life Sciences) was injected and the reporter gene expression was analyzed 10 minutes later. Images and assessment of emitted light were analyzed with the Living Image Software version 4.2.

**ELISpot assay.** Spleen cells from groups of mice (five to seven mice/group) were pooled and tested for the presence of HBcAg-specific T cells. The ability of HBcAg-specific CTLs and Th cells to produce IFN-γ and IL-2 after exposure to different peptides; MGLKFRQL (H-2K<sup>b</sup>, HBcAg-CTL) sequence designed from HBcAg (aa 93–100); PPAYRPPNAPIL (HBcAg-Th) sequence designed from HBcAg (aa 129–140); or 3 peptide pools of 20-mer peptides with 10 aa overlap covering the HBcAg (pool 1: 17 peptides covering aa 1–180, pool 2: 9 peptides covering aa 1–110 and pool 3: 8 peptides covering aa 101–180); recombinant HBcAg-protein; SIINFEKL (OVA aa 257–264, CTL-epitope); ISQAVHAAHAEINEAGR (OVA aa 323–339, Th-epitope); proteins (OVA grade VII); Concanavalin A (ConA) and media was assessed. Production of IFN-γ and IL-2 cytokines was determined by a commercially available enzyme-linked immunospot assay as described previously.<sup>46</sup>

**Quantification of HBcAg-specific CD8<sup>+</sup> T-cell frequencies.** The frequency of HBcAg-specific CD8<sup>+</sup> T cells was analyzed by direct *ex vivo* staining of splenocytes using the HBcAg MHC class I MGLKFRQL (H-2K<sup>b</sup>) Pro5 pentamer (ProImmune, Oxford, UK) exactly as described previously.<sup>25</sup>

**Characterization of polyfunctional T cells.** 5 × 10<sup>5</sup> splenocytes were restimulated for 12 hours in the presence of GolgiPlug (BD Biosciences, San Jose, CA) with HBcAg CTL peptide (5 µg/ml), Th peptide (5 µg/ml), recombinant protein (0.3 µg/ml), and peptide pools (0.3 µg/ml each peptide). Staining was done using Pacific Blue rat anti-mouse CD3, PerCP rat anti-mouse CD8a, APC rat anti-mouse IL-2, FITC rat anti-mouse IFN-γ (Biolegend, San Diego, CA), PE rat anti-mouse CD107a, and PE-Cy7 rat anti-mouse TNF-α antibodies (BD Biosciences). LIVE/DEAD Fixable Aqua Dead Cell Stain Kit (Invitrogen, Paisley, UK) was used as a dead cell marker. Permeabilization of cells was performed using the BD Cytofix/Cytoperm™ Fixation/Permeabilization Kit. Cells were acquired on a LSRFortessa flow cytometer (BD Biosciences) and analyzed using FlowJo 9.6.2 software (TreeStar, Ashland, OR). From a live lymphocyte gate CD8<sup>+</sup> T cells were identified by CD3 versus CD8 staining. These cells were analyzed for cytokine expression (IFN-γ, TNF-α, IL-2) as well as CD107a. Results were given as individual cytokines produced alone and/or in combination

as percent of total CD8<sup>+</sup> T cells. The pie charts represent the proportion of cytokine-secreting CD8<sup>+</sup> T cells that produce one, two, three, or four cytokines/surface markers.

**Detection of HbCag-specific antibodies using ELISA.** Serum from immunized C57BL/6J and HBeAg-Tg mice were tested for mouse IgG antibodies to HbCag. In brief, plates were coated with 1 µg/ml rHbCag in 50 mmol/l sodium carbonate buffer (pH 9.6) overnight at 4 °C. Plates were blocked by incubation with dilution buffer (phosphate-buffered saline, 2% goat serum, 1% BSA) for 1 hour at 37 °C. Mouse serum was added in serial dilutions with a starting dilution of 1:60 and then in serial dilution of either 1:2 or 1:6. Serum antibodies were detected by an alkaline phosphatase-conjugated goat anti-mouse IgG (Sigma A1047) and visualized using p-nitrophenyl phosphate substrate solution. OD was read at 405 nm with a 620 nm background. The cutoff value was set to three times the OD value of a negative (nonimmunized mice) serum sample.

Detection of IgG subclasses (IgG1, IgG2a, IgG2b, and IgG3) (Southern Biotech, Birmingham, AL) was performed in a similar manner as described above with the exception that serum antibodies were detected using subclass-specific anti-mouse horseradish peroxidase-conjugated antibodies and visualized using TMB phosphate citrate substrate solution. OD was read at 450 nm. The cutoff value was set to three times the OD value of a negative (nonimmunized mice) serum sample.

**Immunohistological detection of HbCag in mouse liver sections.** Liver specimens were fixed in 10% phosphate-buffered formalin and subsequently embedded in paraffin. For histopathological evaluation, deparaffinized sections from at least two different liver lobes were stained, for each mouse, with Hematoxylin-Eosin or anti-HbCag antibody. To retrieve antigens, liver sections were boiled in a pressure cooker. For detection of the presence of HbCag-protein in liver tissue, a polyclonal rabbit anti-HbC antibody (Dako B0586, Glostrup, Denmark) was used at a dilution of 1:3,000 in 0.01 mol/l citrate buffer complemented with 2.5% normal horse serum. Following incubation with the primary antibody, an ImmPRESS anti-rabbit Ig peroxidase detection kit was used before visualization using the DAB peroxidase substrate kit (Dako SK-4100) as a chromogen. Sections were counterstained with hematoxylin. The Hematoxylin-Eosin (H&E) staining was performed using standard techniques described in detail elsewhere.

**Immuno-precipitation and western blot analysis for detection of HbCag-protein in mouse livers.** At 72 hours after generation of transient HbCag-protein expression in mice livers by hydrodynamic injection mice were sacrificed and livers harvested for analysis of HbCag-protein by immunoprecipitation and western blot analysis. HbCag-expression was detected in liver homogenates. In brief, 100-mg liver were homogenized in 1 ml RIPA buffer (0.15 mol/l NaCl containing 50 mmol/l Tris, 1% Triton X-100, 1% Na-deoxycholate, and 1% sodium dodecyl sulfate (SDS)). The homogenates were immunoprecipitated with protein-A sepharose and polyclonal mouse anti-HbC overnight at 4 °C. Samples were diluted in SDS sample buffer, heated at 100 °C for 5 minutes before SDS-PAGE analysis on 4–12% Bis-Tris gel (Life Technologies) followed by ET onto nitrocellulose membranes using the iBlot (Life Technologies). HbCag-proteins were detected using a polyclonal rabbit anti-HbC (B0586 Dako) antibody, diluted 1:1,500. Chemiluminescence-linked Western blot kit (WesternBreeze WB7106; Life Technologies) was used for the detection of HbCag according to the manufacturer's protocol. Chemiluminescent signals were detected using the G:BOX Chemi XX6 gel documentation system (Syngene, Cambridge, UK).

**Statistical analysis.** GraphPad InStat 3, Macintosh and Microsoft Excel 2008, Macintosh was used for statistical comparison of experimental data. Kinetic measurements were compared using the AUC (Excel). Parametrical data were compared using the ANOVA and nonparametric data with Mann-Whitney *U*-test.

## SUPPLEMENTARY MATERIAL

**Figure S1.** Loss of *in vivo* functional T cell responses six weeks after a single immunization.

## ACKNOWLEDGMENTS

We kindly thank Darrell L. Peterson, Virginia Commonwealth University (Richmond, VA) for providing the recombinant HbCag protein and Marit Bjorn-Holm for preparing and performing the histological examination of mouse livers. The study was supported by grants from the Swedish Research Council (K2012-99X-22017-01-3 (L.F., M.S.)), the Swedish Cancer Society (M.S.), Stockholm County Council (M.S.), Vinnova (M.S.), the Royal Swedish Academy of Sciences (G.A.), Lars Hierta Memorial Foundation (G.A.), the Magnus Bergwalls Foundation (G.A.), Karolinska Institutet (L.F., M.S., G.A.) Karolinska Institutet/Södertörn University (postdoctoral grant to A.B., G.A.), ChronTech Pharma AB and private donations. M.S. is founder, paid consultant, and board member of ChronTech Pharma AB. L.F. and G.A. are paid consultants of ChronTech Pharma AB. D.R.M. is a founder of VLP Biotech, Inc. A.B. reports no potential conflict of interest.

## REFERENCES

- Lok, AS (2013). Hepatitis: Long-term therapy of chronic hepatitis B reverses cirrhosis. *Nat Rev Gastroenterol Hepatol* **10**: 199–200.
- Hosaka, T, Suzuki, F, Kobayashi, M, Seko, Y, Kawamura, Y, Sezaki, H *et al.* (2013). Long-term entecavir treatment reduces hepatocellular carcinoma incidence in patients with hepatitis B virus infection. *Hepatology* **58**: 98–107.
- Zoulim, F and Locarnini, S (2009). Hepatitis B virus resistance to nucleos(t)ide analogues. *Gastroenterology* **137**: 1593–608.e1.
- Whalley, SA, Murray, JM, Brown, D, Webster, GJ, Emery, VC, Dusheiko, GM *et al.* (2001). Kinetics of acute hepatitis B virus infection in humans. *J Exp Med* **193**: 847–854.
- Webster, GJ, Reignat, S, Maini, MK, Whalley, SA, Ogg, GS, King, A *et al.* (2000). Incubation phase of acute hepatitis B in man: dynamic of cellular immune mechanisms. *Hepatology* **32**: 1117–1124.
- Maini, MK, Boni, C, Lee, CK, Larrubia, JR, Reignat, S, Ogg, GS *et al.* (2000). The role of virus-specific CD8(+) cells in liver damage and viral control during persistent hepatitis B virus infection. *J Exp Med* **191**: 1269–1280.
- Marinos, G, Torre, F, Chokshi, S, Hussain, M, Clarke, BE, Rowlands, DJ *et al.* (1995). Induction of T-helper cell response to hepatitis B core antigen in chronic hepatitis B: a major factor in activation of the host immune response to the hepatitis B virus. *Hepatology* **22**(4 Pt 1): 1040–1049.
- Löhr, HF, Weber, W, Schlaak, J, Goergen, B, Meyer zum Buschenfelde, KH and Gerken, G (1995). Proliferative response of CD4+ T cells and hepatitis B virus clearance in chronic hepatitis with or without hepatitis B e-minus hepatitis B virus mutants. *Hepatology* **22**: 61–68.
- Penna, A, Chisari, FV, Bertoletti, A, Missale, G, Fowler, P, Giuberti, T *et al.* (1991). Cytotoxic T lymphocytes recognize an HLA-A2-restricted epitope within the hepatitis B virus nucleocapsid antigen. *J Exp Med* **174**: 1565–1570.
- Boni, C, Bertoletti, A, Penna, A, Cavalli, A, Pilli, M, Urbani, S *et al.* (1998). Lamivudine treatment can restore T cell responsiveness in chronic hepatitis B. *J Clin Invest* **102**: 968–975.
- Boni, C, Laccabue, D, Lampertico, P, Giuberti, T, Viganò, M, Schivazappa, S *et al.* (2012). Restored function of HBV-specific T cells after long-term effective therapy with nucleos(t)ide analogues. *Gastroenterology* **143**: 963–73.e9.
- Gish, R, Jia, JD, Locarnini, S and Zoulim, F (2012). Selection of chronic hepatitis B therapy with high barrier to resistance. *Lancet Infect Dis* **12**: 341–353.
- Tavis, JE, Gehring, AJ and Hu, Y (2013). How further suppression of virus replication could improve current HBV treatment. *Expert Rev Anti Infect Ther* **11**: 755–757.
- Mancini-Bourgine, M, Fontaine, H, Scott-Algara, D, Pol, S, Bréchet, C and Michel, ML (2004). Induction or expansion of T-cell responses by a hepatitis B DNA vaccine administered to chronic HBV carriers. *Hepatology* **40**: 874–882.
- Scott-Algara, D, Mancini-Bourgine, M, Fontaine, H, Pol, S and Michel, ML (2010). Changes to the natural killer cell repertoire after therapeutic hepatitis B DNA vaccination. *PLoS One* **5**: e8761.
- Habersetzer, F, Honnet, G, Bain, C, Maynard-Muet, M, Leroy, V, Zarski, JP *et al.* (2011). A poxvirus vaccine is safe, induces T-cell responses, and decreases viral load in patients with chronic hepatitis C. *Gastroenterology* **141**: 890–899.e1.
- Weiland, O, Ahlén, G, Diepolder, H, Jung, MC, Levander, S, Fons, M *et al.* (2013). Therapeutic DNA vaccination using *in vivo* electroporation followed by standard of care therapy in patients with genotype 1 chronic hepatitis C. *Mol Ther* **21**: 1796–1805.
- Godon, O, Fontaine, H, Kahi, S, Meritet, J, Scott-Algara, D, Pol, S *et al.* (2014). Immunological and antiviral responses after therapeutic DNA immunization in chronic hepatitis B patients efficiently treated by analogues. *Mol Ther* **22**: 675–684.
- Boni, C, Fiscaro, P, Valdatta, C, Amadei, B, Di Vincenzo, P, Giuberti, T *et al.* (2007). Characterization of hepatitis B virus (HBV)-specific T-cell dysfunction in chronic HBV infection. *J Virol* **81**: 4215–4225.
- Thimme, R, Wieland, S, Steiger, C, Ghayee, J, Reimann, KA, Purcell, RH *et al.* (2003). CD8(+) T cells mediate viral clearance and disease pathogenesis during acute hepatitis B virus infection. *J Virol* **77**: 68–76.
- Webster, GJ, Reignat, S, Brown, D, Ogg, GS, Jones, L, Seneviratne, SL *et al.* (2004). Longitudinal analysis of CD8+ T cells specific for structural and nonstructural hepatitis

## HBV Vaccine Induces T-cell Immunity in HBV-Tg Mice

- B virus proteins in patients with chronic hepatitis B: implications for immunotherapy. *J Virol* **78**: 5707–5719.
22. Seder, RA, Darrah, PA and Roederer, M (2008). T-cell quality in memory and protection: implications for vaccine design. *Nat Rev Immunol* **8**: 247–258.
  23. Badr, G, Bédard, N, Abdel-Hakeem, MS, Trautmann, L, Willems, B, Villeneuve, JP *et al.* (2008). Early interferon therapy for hepatitis C virus infection rescues polyfunctional, long-lived CD8+ memory T cells. *J Virol* **82**: 10017–10031.
  24. Nyström, J, Chen, A, Frelin, L, Ahlén, G, Koh, S, Brass, A *et al.* (2010). Improving on the ability of endogenous hepatitis B core antigen to prime cytotoxic T lymphocytes. *J Infect Dis* **201**: 1867–1879.
  25. Chen, A, Ahlén, G, Brenndörfer, ED, Brass, A, Holmström, F, Chen, M *et al.* (2011). Heterologous T cells can help restore function in dysfunctional hepatitis C virus nonstructural 3/4A-specific T cells during therapeutic vaccination. *J Immunol* **186**: 5107–5118.
  26. Milich, DR, Jones, JE, Hughes, JL, Price, J, Raney, AK and McLachlan, A (1990). Is a function of the secreted hepatitis B e antigen to induce immunologic tolerance in utero? *Proc Natl Acad Sci USA* **87**: 6599–6603.
  27. Milich, DR, McLachlan, A, Raney, AK, Houghten, R, Thornton, GB, Maruyama, T *et al.* (1991). Autoantibody production in hepatitis B e antigen transgenic mice elicited with a self T-cell peptide and inhibited with nonself peptides. *Proc Natl Acad Sci USA* **88**: 4348–4352.
  28. Milich, DR, Schödel, F, Peterson, DL, Jones, JE and Hughes, JL (1995). Characterization of self-reactive T cells that evade tolerance in hepatitis B e antigen transgenic mice. *Eur J Immunol* **25**: 1663–1672.
  29. Rossol, S, Marinos, G, Carucci, P, Singer, MV, Williams, R and Naoumov, NV (1997). Interleukin-12 induction of Th1 cytokines is important for viral clearance in chronic hepatitis B. *J Clin Invest* **99**: 3025–3033.
  30. Kim, JJ, Ayyavoo, V, Bagarazzi, ML, Chattergoon, MA, Dang, K, Wang, B *et al.* (1997). *In vivo* engineering of a cellular immune response by coadministration of IL-12 expression vector with a DNA immunogen. *J Immunol* **158**: 816–826.
  31. Ahlen, G, Nyström, J, Pult, I, Frelin, L, Hultgren, C and Sällberg, M (2005). *In vivo* clearance of hepatitis C virus nonstructural 3/4A-expressing hepatocytes by DNA vaccine-primed cytotoxic T lymphocytes. *J Infect Dis* **192**: 2112–2116.
  32. Lazdina, U, Alheim, M, Nyström, J, Hultgren, C, Borisova, G, Sominskaya, I *et al.* (2003). Priming of cytotoxic T cell responses to exogenous hepatitis B virus core antigen is B cell dependent. *J Gen Virol* **84**(Pt 1): 139–146.
  33. Kuhöber, A, Pudollek, HP, Reifenberg, K, Chisari, FV, Schlicht, HJ, Reimann, J *et al.* (1996). DNA immunization induces antibody and cytotoxic T cell responses to hepatitis B core antigen in H-2b mice. *J Immunol* **156**: 3687–3695.
  34. Milich, DR, Peterson, DL, Schödel, F, Jones, JE and Hughes, JL (1995). Preferential recognition of hepatitis B nucleocapsid antigens by Th1 or Th2 cells is epitope and major histocompatibility complex dependent. *J Virol* **69**: 2776–2785.
  35. Milich, DR, Schödel, F, Hughes, JL, Jones, JE and Peterson, DL (1997). The hepatitis B virus core and e antigens elicit different Th cell subsets: antigen structure can affect Th cell phenotype. *J Virol* **71**: 2192–2201.
  36. Frelin, L, Wahlström, T, Tucker, AE, Jones, J, Hughes, J, Lee, BO *et al.* (2009). A mechanism to explain the selection of the hepatitis e antigen-negative mutant during chronic hepatitis B virus infection. *J Virol* **83**: 1379–1392.
  37. Obeng-Adjai, N, Choo, DK, Saini, J, Yan, J, Pankhong, P, Parikh, A *et al.* (2012). Synthetic DNA immunogen encoding hepatitis B core antigen drives immune response in liver. *Cancer Gene Ther* **19**: 779–787.
  38. Chong, SY, Egan, MA, Kutzler, MA, Megati, S, Masood, A, Roopchand, V *et al.* (2007). Comparative ability of plasmid IL-12 and IL-15 to enhance cellular and humoral immune responses elicited by a SIVgag plasmid DNA vaccine and alter disease progression following SHIV(89.6P) challenge in rhesus macaques. *Vaccine* **25**: 4967–4982.
  39. Kalams, SA, Parker, S, Jin, X, Elizaga, M, Metch, B, Wang, M *et al.*; NIAID HIV Vaccine Trials Network. (2012). Safety and immunogenicity of an HIV-1 gag DNA vaccine with or without IL-12 and/or IL-15 plasmid cytokine adjuvant in healthy, HIV-1 uninfected adults. *PLoS One* **7**: e29231.
  40. Babiuk, S, Baca-Estrada, ME, Foldvari, M, Middleton, DM, Rabussay, D, Widera, G *et al.* (2004). Increased gene expression and inflammatory cell infiltration caused by electroporation are both important for improving the efficacy of DNA vaccines. *J Biotechnol* **110**: 1–10.
  41. Ahlén, G, Söderholm, J, Tjelle, T, Kjeker, R, Frelin, L, Höglund, U *et al.* (2007). *In vivo* electroporation enhances the immunogenicity of hepatitis C virus nonstructural 3/4A DNA by increased local DNA uptake, protein expression, inflammation, and infiltration of CD3+ T cells. *J Immunol* **179**: 4741–4753.
  42. Kosinska, AD, Zhang, E, Johrden, L, Liu, J, Seiz, PL, Zhang, X *et al.* (2013). Combination of DNA prime–adenovirus boost immunization with entecavir elicits sustained control of chronic hepatitis B in the woodchuck model. *PLoS Pathog* **9**: e1003391.
  43. Chen, H, Chuai, X, Deng, Y, Wen, B, Wang, W, Xiong, S *et al.* (2012). Optimisation of prime-boost immunization in mice using novel protein-based and recombinant vaccinia (Tiantan)-based HBV vaccine. *PLoS One* **7**: e43730.
  44. Milich, DR, Chen, M, Schödel, F, Peterson, DL, Jones, JE and Hughes, JL (1997). Role of B cells in antigen presentation of the hepatitis B core. *Proc Natl Acad Sci USA* **94**: 14648–14653.
  45. Sällberg, M, Rudén, U, Magnusius, LO, Norrby, E and Wahren, B (1991). Rapid “tea-bag” peptide synthesis using 9-fluorenylmethoxycarbonyl (Fmoc) protected amino acids applied for antigenic mapping of viral proteins. *Immunol Lett* **30**: 59–68.
  46. Ahlén, G, Holmström, F, Gibbs, A, Alheim, M and Frelin, L (2014). Long-term functional duration of immune responses to HCV NS3/4A induced by DNA vaccination. *Gene Ther* **21**: 739–750.



This work is licensed under a Creative Commons Attribution-NonCommercial-ShareAlike 3.0 Unported License. The images or other third party material in this article are included in the article's Creative Commons license, unless indicated otherwise in the credit line; if the material is not included under the Creative Commons license, users will need to obtain permission from the license holder to reproduce the material. To view a copy of this license, visit <http://creativecommons.org/licenses/by-nc-sa/3.0/>